

# Voltammetric Studies of Lead at a New Carbon Paste Microelectrode Modified with N(2-isopropylphenyl)-2-thioimidazole and its Trace Determination in Water by Square Wave Voltammetry

Gaber A. M. Mersal<sup>1,2,\*</sup> and M. M. Ibrahim<sup>1,3</sup>

<sup>1</sup> Chemistry Department, Faculty of Science, Taif University, 888 Taif, Kingdom of Saudi Arabia

<sup>2</sup> Chemistry Department, Faculty of Science, South Valley University, Qena, Egypt

<sup>3</sup> Chemistry Department, Faculty of Science, Kafr El-Sheikh University, Kafr El-Sheikh 33516, Egypt

\*E-mail: [gamersal@yahoo.com](mailto:gamersal@yahoo.com)

Received: 15 December 2011 / Accepted: 29 February 2013 / Published: 1 April 2013

---

The electrocatalytic oxidation of lead(II) was investigated on a novel carbon paste microelectrode modified with a thione-containing ligand namely, N(2-isopropylphenyl)-2-thioimidazole (Hmim). The carbon paste electrode modified with N(2-isopropylphenyl)-2-thioimidazole (CPME-Hmim) was characterized using scanning electron microscope (SEM) and cyclic voltammetry (CV). The electrochemical behavior of lead(II) ions at the modified electrode surface showed one anodic peak at -0.43 V and one cathodic peak at -0.55 V with a separation peak potential of 120 mV. The anodic and cathodic peak current heights of lead(II) ions in the case of CPME-Hmim was much higher than that in the case of the unmodified one, CPE. This is due to the accumulation of lead(II) ions at the surface of CPME-Hmim, forming the monomeric lead(II) complex [(Hmim)<sub>2</sub>Pb(NO<sub>3</sub>)<sub>2</sub>]. Square wave voltammetry was used for the electrochemical determination of lead(II) ions at CPME-Hmim with optimum conditions and calibration curve (analytical equation:  $y = -2.129 \times 10^{-5} + 1.847x$ ). The obtained results showed a recovery ranged between 98.67-106.11%. The lead(II) ions was determined in different water samples and the obtained results were compared with the data obtained from the ICP-AES instrument.

---

**Keywords:** Lead, N(2-isopropylphenyl)-2-thioimidazole, Carbon paste microelectrode, Cyclic voltammetry

## 1. INTRODUCTION

Environmental pollution is one of the most serious problems facing our recent world. Trace elements, especially heavy metals, are considered to be one of the main sources of pollution in the

environment. Lead is one of the most dangerous environmental pollutants where it has a strong chemical toxicity effect even in the presence of low concentrations. Lead is highly toxic to human and animal organs such nervous, immune, reproductive and gastrointestinal systems. The main source of lead in the environment is due to the old housing especially houses painted with products containing lead as pigment and soil contaminated by lead residues from gasoline and industrial processes. Human activities such as mining, smelting, refining, manufacturing, and recycling, lead finds its way into the air, water, and the surface soil. Lead –containing manufactured products such as gasoline, paint, painting inks, lead water pipes, lead –glazed pottery, lead –soldered cans and battery casings also contribute to the lead burden. Lead in contaminated soil and dust can find its way into food and water supply.

So it is very important to find a very sensitive and selective method for the determination of trace levels of lead in the environment. Different techniques were used for trace lead analysis such as spectroscopic methods especially graphite furnace atomic adsorption spectroscopy (GF-AAS), and inductively coupled plasma mass spectroscopy (ICP-MS)[1-6]. These methods have excellent sensitivity and good selectivity, but have different drawbacks such as time consuming used for analysis and very expensive instruments are required. Electrochemical methods including stripping voltammetric techniques such as anodic stripping voltammetry, cathodic stripping voltammetry, square wave voltammetry and differential pulse voltammetry have recognized powerful tools for measuring trace analysis. It have shown different advantages such as speed of analysis, higher selectivity and sensitivity, low coast, easy operation and the ability of analyzing element speciation. Different working electrodes were used for the voltammetric determination of lead such as hanging mercury drop electrode (HMDE) [7-12], mercury film electrode [13], gold electrode [14] gold screen printed electrode [15], Bismuth oxide screen printed electrode [16], and renovated silver ring electrode [17]. Chemically modified electrodes have been develop the recent years for the electrochemical determination of heavy metals due to different advantages such as easy manufacture, no poison, renewable, fast response, high selectivity, low detection limit, stable in various solvent, longer life time and low cost.

A number of chemically modified electrodes were developed for the electrochemical; determination of lead such as bismuth glassy carbon composite electrode [18], hydroxylapatite modified carbon ionic liquid electrode [19], cyclodextrin modified gold electrode [20], kaolin modified platinum electrode [21], cyclam-modified graphite felt electrodes [22], hydroxylapatite modified platinum electrode [23], 1-(2-pyridylazo)-2-naphthol modified screen printed carbon electrode [24], calixarene modified screen printed carbon electrode [25], anthraquinone improved Na-montmorillonite nanoparticles glassy carbon electrode [26], Langmuir – Blodgett film of p-tert-butylthiacalix[4]arene modified glassy carbon electrode [27], screen printed carbon electrode modified with bismuth oxide electrode [28], glassy carbon electrode modified with mercury [29] and chemically carbon paste electrodes. Carbon paste electrode (CPE) is one of the most popular chemically modified electrodes used with voltammetric techniques. This electrode prepared by mixing a graphite powder with a suitable binder and a material known as a modifier that improves the selectivity of the prepared electrode. In the literature survey some modifiers were used with carbon paste electrode for the electrochemical determination of lead, such as zeolite [30], hydroxyapatite [31], modified with SBA-

15 nanostructured silica organofunctionalised with 2-benzothiazolethiol [32], carbamoylphosphonic acid [33], diacetyldioxime [34], 1,4-bis(prop-2'-enyloxy)-9,10-anthraquinone [35] and Chitosan [36]. Lead (II) complexes with sulfur donor atom ligands have been studied actively during the last few decades due to their significant structural diversity and multiple applications for these compounds [37]. In order to increase both the selectivity and sensitivity for the electrochemical determination of lead(II) ions, a thione-containing ligand, namely, N(2-isopropylphenyl)-2-thioimidazole was selected for the modification of carbon paste microelectrode. The present work aimed to the determination of lead(II) ions in different water samples and the obtained results were compared with the data obtained from the ICP-AES instrument.

## 2. EXPERIMENTAL

### 2.1. Chemicals

All reagents were of commercial grade materials and were used without further purification. Graphite powder, paraffin wax and lead (II) nitrate were obtained from Sigma-Aldrich.  $\text{H}_3\text{BO}_3$ ,  $\text{H}_3\text{PO}_4$ ,  $\text{NaH}_2\text{PO}_4$ ,  $\text{Na}_2\text{HPO}_4$ ,  $\text{CH}_3\text{COOH}$ ,  $\text{HCl}$ , and  $\text{NaOH}$  were obtained from Merck. Double distilled water was used for the preparation of solutions.

### 2.2. Synthesis of N(2-isopropylphenyl)-2-thioimidazole (Hmim)

A solution of 2-isopropyl-butylaniline (27.0 g, 0.2 mol) in dry diethyl ether (40 mL) was slowly added to a solution containing a mixture of  $\text{NaNH}_2$  (7.8 g, 0.12 mol) and bromoacetal (39.4 g, 0.1 mol) in 60 mL dry diethyl ether. The resulting solution was stirred for 2h under stream of nitrogen. Then, the solvent was removed in vacuo, and the residue was heated to 120 °C overnight for completion the reaction. Ethanol (30 mL) was carefully added, followed by water (20 mL). The resulting solution was stirred for one 1h. The remained solid material was extracted from n-hexane and dried with magnesium sulfate, giving N-(2,2-diethoxyethyl)-isopropylaniline, which was mixed with potassium thiocyanate (14.9 g, 0.153 mol) in ethanol (130 mL). Then add 75 mL ( $\text{HCl}$ , 2N). The reaction mixture was refluxed for 24 hrs. The solvent was removed by rotatory evaporator. A hot water (500 ml) was added to the residue with stirring. Cool down and a raw product was obtained as pale yellow solid, filtered, dried, and crystallized from ethanol by using activated charcoal. N(2-isopropylphenyl)-2-thioimidazole was obtained as white crystals. Yield: 59.3%. M. p. 246 °C (dec). Anal. Calcd. for  $\text{C}_{12}\text{H}_{14}\text{N}_2\text{S}$  (218.32): C, 66.02; H, 6.46; N, 12.83; S, 14.69. Found: C, 65.22; H, 6.67; N, 12.45; S, 14.81.  $^1\text{H-NMR}$  ( $\text{CDCl}_3$ , 298 K, TMS):  $\delta$  1.12 [d, J = 6.9 Hz, 6H,  $\text{CH}_3$ ], 2.61(m, J = 6.7 Hz, 2H,  $\text{CH}$ ], 6.64 [d, J = 2.2 Hz, 1H,  $\text{H}^3$ -thioimidazole], 6.85 [d J = 2.2 Hz, 1H,  $\text{H}^2$ -thioimidazole], 7.29-7.42 [m, 4H,  $\text{C}_6\text{H}_5$ ], 12.20 ppm [s, 1H,  $\text{NH}$ ].  $^{13}\text{C NMR}$  ( $\text{CDCl}_3$ , 298 K, TMS):  $\delta$  = 22.6 ( $\text{CH}_3$  (ipr)), 24.4 ( $\text{CH}_3$  (ipr)), 28.4 ( $\text{CH}$  ((ipr))), 119.5 ( $\text{C}^3$ -thioimidazole), 119.8 ( $\text{C}^2$ -thioimidazole), 124.1, 129.7 ( $\text{C}_6\text{H}_5$  (1,4)), 134.4 ( $\text{C}_6\text{H}_5$  (3,5)), 146.7 ( $\text{C}_6\text{H}_5$  (2,6)), and 165.9 ppm ( $\text{C}^1$ -thioimidazole). IR

(KBr),  $\nu(\text{cm}^{-1})$ : 3097 (s, br, NH), 1573 (s,  $-\text{C}=\text{C}- + \text{C}=\text{N}$ ), 1474 (s, Thioamide I), 1295 (vs, Thioamide II), 1137 (m, thioamide III), 775 & 725 (s, Thioamide IV), 683 [m,  $\delta$  (C-S)], and 533 [s,  $\pi$  (C=S)].

### 2.3. Synthesis of Bis(*N*-isopropyl-2-thioimidazolyl)bis(nitrato)lead(II)

A warm solution of  $\text{Pb}(\text{NO}_3)_2$  (132 mg, 0.4 mmol) in 10 mL of methanol was added to a warm solution of the ligand Hmim (175 mg, 0.8 mmol) in 10 mL methanol. The resulting mixed solution was stirred for 6 h at room temperature. The volume of the solution was reduced to 10 mL in vacuo. Colorless crystals were obtained by slow evaporation of methanolic solution of the complex. Anal. Calcd. For  $\text{C}_{24}\text{H}_{28}\text{N}_6\text{S}_2\text{O}_6\text{Pb}$  (767.84): C, 37.54; H, 3.68; N, 10.94; S, 8.35. Found: C, 36.67; H, 3.77; N, 10.44; S, 8.56. IR (KBr),  $\nu(\text{cm}^{-1})$ : 3116 (s, br, NH), 1585 (s,  $-\text{C}=\text{C}- + \text{C}=\text{N}$ ), 1488 (s, Thioamide I), 1299 (vs, Thioamide II), 1145 (m, thioamide III), 761 & 688 (s, Thioamide IV), 687 [m,  $\delta$  (C-S)], and 522 [s,  $\pi$  (C=S)].

### 2.4. Preparation of Unmodified Carbon Paste Electrode (CPE) and Carbon Paste Modified by *N*(2-isopropylphenyl)-2-thioimidazole (CPME-Hmim)

Unmodified carbon paste electrode was prepared as mentioned before [38] by mixing 65% graphite powder and 35% paraffin wax. Paraffin wax was heated till melting and then, mixed very well with graphite powder to produce a homogeneous paste. The resulted paste was then packed into the end of an insulin syringe (i.d.: 2mm). External electrical contact was established by forcing a copper wire down the syringe. CPE modified with Hmim was prepared by mixing 60% graphite powder and 30% paraffin wax with 1, 3, 5, 10% Hmim. The surface of the electrode was polished with a piece of weighting paper and then rinsed with distilled water thoroughly.

### 2.5. Physical measurements

Infrared spectral measurements for the free ligand and its lead(II) complex  $[(\text{Hmim})_2\text{Pb}(\text{NO}_3)_2]$  were recorded in KBR pellets using FT-IR Prestige-21 Shimadzu, in the range of 400-4000  $\text{cm}^{-1}$ . Raman spectra were obtained as powder in glass capillaries on a Nicolet FT Raman 950 spectrophotometer. The spectra were recorded at room temperature with a germanium detector, maintained at liquid nitrogen temperature and using 1064.0 nm radiation, generated by a Nd-YAG laser with a resolution of 2  $\text{cm}^{-1}$ .  $^1\text{H}$ - $^{13}\text{C}$  NMR spectra were taken for the ligand and its complexes using Varian 400-NMR spectrophotometer. The  $^1\text{H}$ -NMR spectra were recorded employing TMS as a reference and  $\text{CDCl}_3$  as a solvent at ambient temperature. Thermal analyses of the complexes were recorded on Netzsch STA 449F3 with system interface device in the atmosphere of nitrogen. The temperature scale of the instrument was calibrated with high purity calcium oxalate. Accurately 5 mg of pure sample was subjected for dynamic TG scans at heating rate of 10  $^\circ\text{C min}^{-1}$ . Scanning electron microscopy (SEM; JEOL JSM-6700F), was used to characterize the morphology of the bare carbon paste (CPE) and the modified carbon paste electrode (CPME-Hmim).

## 2.6. Electrochemical Measurements

Cyclic voltammetry (CV) and square wave voltammetry were performed using an Autolab potentiostat PGSTAT 302 (Eco Chemie, Utrecht, The Netherlands) driven by the General purpose Electrochemical systems data processing software (GPES, software version 4.9, Eco Chemie). Electrochemical cell with three electrodes was used; unmodified carbon paste electrode or carbon paste electrode modified with N(2-isopropylphenyl)-2-thioimidazole was used as a working electrode, Ag/AgCl was used as a reference electrode while platinum wire was used as a counter electrode. The pH values were measured using a Metrohm pH-meter with a combined glass electrode. pH values were adjusted using 1.0 M NaOH solution.

## 3. RESULTS AND DISCUSSIONS

### 3.1. Characterization of the ligand N(2-isopropylphenyl)-2-thioimidazole (Hmim) and [(Hmim)<sub>2</sub>Pb(NO<sub>3</sub>)<sub>2</sub>]

The reaction of the ligand Hmim with Pb(NO<sub>3</sub>)<sub>2</sub> in 2:1 molar ratio in hot methanol, readily produced the crystalline complex [Pb(Hmim)<sub>2</sub>(NO<sub>3</sub>)<sub>2</sub>] in a good yield. The elemental analysis of this complex confirmed its stoichiometry and its physical properties are in accordance with the proposed structure. In order to establish the mode of its coordination, we have examined its IR, Raman, and <sup>1</sup>H NMR spectra as well as thermal analysis. The IR spectrum of [(Hmim)<sub>2</sub>Pb(NO<sub>3</sub>)<sub>2</sub>] shows the absence of ν(SH) band at ~2500 cm<sup>-1</sup> and the presence of ν(NH) band in the range of 3097–3116 cm<sup>-1</sup>, as well as shifts to lower frequency in the ν(C=S) absorption to 522 cm<sup>-1</sup>. This clearly indicates that the ligand is coordinated via the thione sulfur atom [39]. These shifts may result from (i) changes in the electronic state where the C=S bond loses some of its double bond character when the ligand coordinates via the thione sulfur and (ii) hydrogen bond effects, where it is a common feature of 1-methylimidazoline-2(3H)-thione complexes in which the thioamide proton (N-H) of the molecule acts as an effective H-bond donor atom [40]. All of the thioamide bands are shifted to some degree, but the most significant change is that observed in the thioamide IV bands, which have the largest shift to lower frequency [41–42]. The thioamide IV band is affected with the bands in the free ligand (775 and 725 cm<sup>-1</sup>), which are replaced by a sharp band at 761 and 688 cm<sup>-1</sup> for [(Hmim)<sub>2</sub>Pb(NO<sub>3</sub>)<sub>2</sub>]. The IR spectra also showed the NO<sub>3</sub><sup>-</sup> absorption at 1384 cm<sup>-1</sup>, which is not found in the ligand itself. The bands below 500 cm<sup>-1</sup>, to angular deformation and Pb–S stretching modes. These shifts may result from changes in the electronic state where the C=S bond loses some of its double bond character when the ligand coordinates via the thione sulfur. The shifts in the bands between the free ligand and the complex result from electronic shifts within the ligand. Information about the low frequency Pb(NO<sub>3</sub>)<sub>2</sub> and Pb(II)–S(thionate) vibrations can be obtained by using Raman spectroscopy. From Raman spectra, the bands of most interest are the ones formed upon complexation, which must therefore be the result of lead(II)–N/S bonding. The absence of the weak SH signals of the thiol form of the ligand and the complex confirms that the coordination of the ligand in the solid state takes place only through the sulfur atom. This observation has been further confirmed [43] for the complexation of thiourea (TU) with HgCl<sub>2</sub>,

forming a complex of the formula  $[\text{Hg}(\text{TU})_2\text{Cl}_2]$ . The thermal analysis of the ligand Hmim indicates that its decomposition proceeds in one step. The TG-DTG thermogram of the ligand exhibits an endothermic event at around  $290^\circ\text{C}$  accompanied by a mass loss of 95.9 % (Calc. 96.72 %), assignable for the removal the whole molecule Hmim, forming carbon as a residual product.

### 3.2. Characterization of CPE and CPME-Hmim

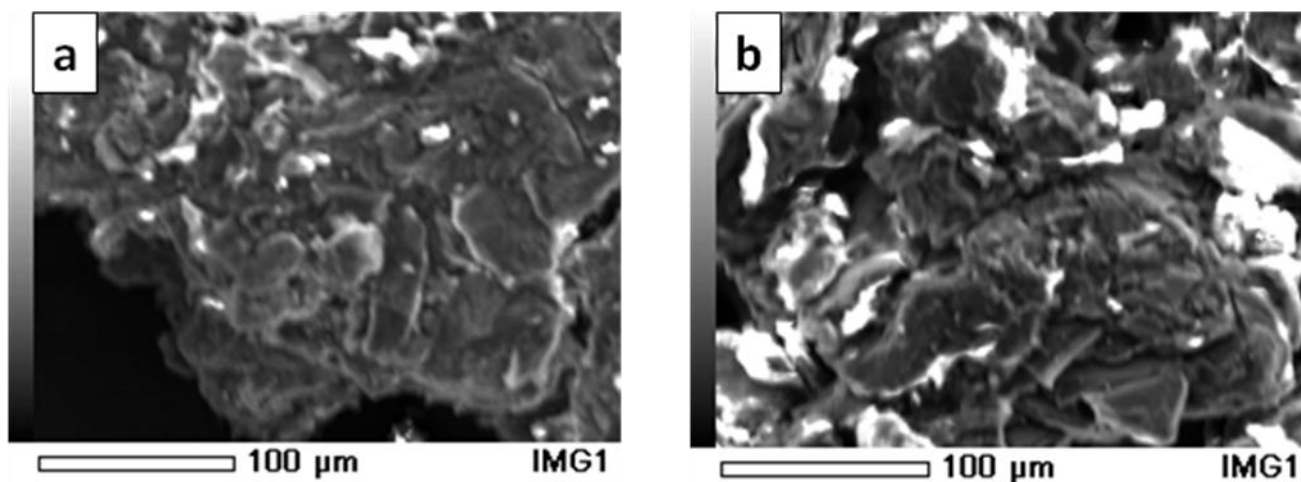


**Figure 1.** SEM for (a) CPE and (b) CPME-Hmim

Scanning electron microscopy (SEM) was used to characterize the morphology of the bare CPE and CPME-Hmim. Fig. 1 presents the SEM for the prepared electrodes. The SEM images of the bare CPE (Fig.1a) showed a microstructure with a discontinuous grain growth with a large unclear crystal structure. Also the surface structure of the bare CPE showed that the graphite particles are covered by a very thin film of paraffin wax. The elemental analysis by EDEX was carried out to evaluate material composition of the prepared electrodes. The EDEX analysis showed that the bare CPE consisted of 100% of carbon and no other elements were appeared. Fig. 1b shows that the surface of CPME-Hmim is relatively homogeneous and more smoother than the bare CPE. The EDEX analysis for a CPME-Hmim showed that the electrode contains carbon by about 79.75%, S by 11.4% and traces from Si (0.38%).

### 3.3. Cyclic voltammetric measurements

Cyclic voltammetry was used to study the electrochemical behavior of Pb(II) at a CPME-Hmim in the absence and presence of Pb(II) ions. The electrochemical behavior of the prepared electrodes was examined in a potential range from - 1.4 to + 1.5 V (vs. Ag/AgCl) for a bare CPE and from -1.5 to 0.0 V (vs. Ag/AgCl) for a CPME-Hmim using a potential scan rate of  $100\text{ mV s}^{-1}$ . The cyclic voltammogram for a bare CPE in the absence of Pb(II) did not show any signals even in the forward or

in the reverse scan. Fig. 2 showed the cyclic voltammogram for a CPE and CPME-Hmim in the presence of  $5 \times 10^{-4}$  M Pb(II) using 0.1 M HCl as a supporting electrolyte.

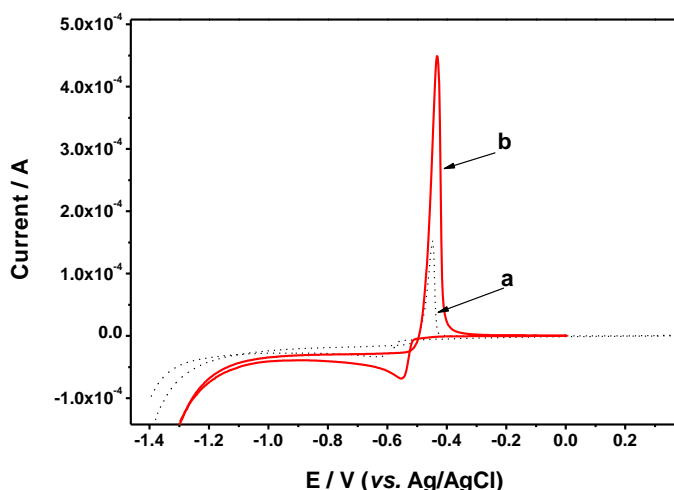
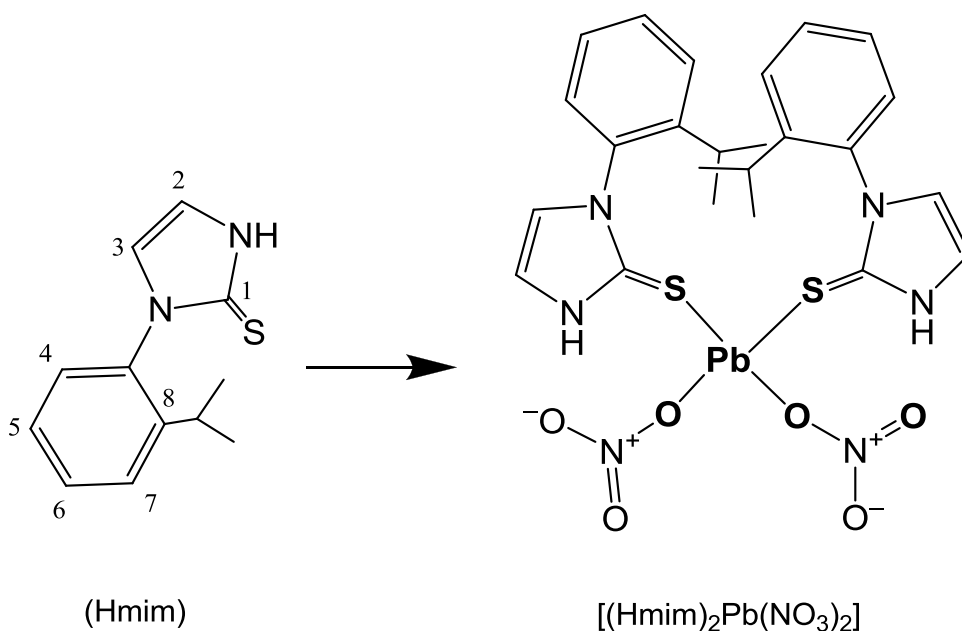


**Figure 2.** Cyclic voltammograms for  $5 \times 10^{-4}$  M Pb(II) ions at (a) CPE and (b) CPME-Hmim.

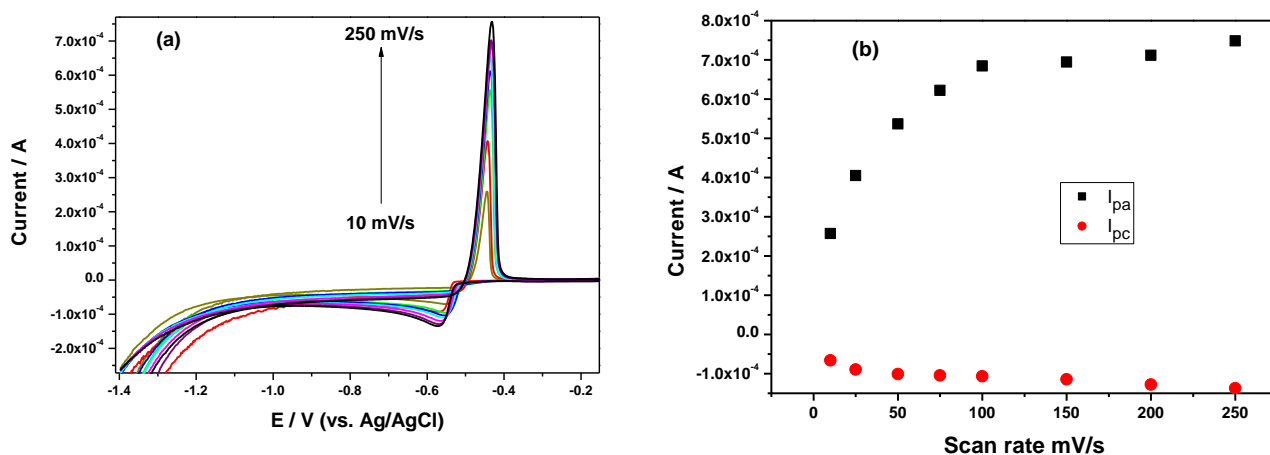
At a bare CPE, Pb(II) showed one quasi reversible reaction, one oxidation peak was appeared at - 0.43 V in the forward scan and another reduction peak was appeared at - 0.64 V at the reverse scan, with a 190 mV separation peak potential ( $\Delta E_p$ ) was obtained. The quasi reversible reaction is attributed to the oxidation of Pb to Pb(II) ions. For a CPME-Hmim also showed anodic peak at - 0.43 V in the forward scan and a small cathodic peak was observed at - 0.55V in the reverse scan with a 120 mV  $\Delta E_p$ . As  $\Delta E_p$  is a function of the rate of electron transfer, the lower  $\Delta E_p$ , the higher electron transfer rate. The results obtained greatly improved the voltammetric response of Pb(II) at CPME-Hmim reflected by the enlargement of peak current and the decrease of peak potential ( $\Delta E_p = 120$  mV). This indicates that the surface property of the modified electrode has been significantly changed. From Fig. 2B it is clear that the anodic peak current for Pb(II) in the presence of a CPME-Hmim is much higher than the peak current of Pb(II) in case of a bare CPE. This enhancement in the peak current due to the increscent of Pb(II) in the electrode surface by the complex formation between Pb(II) and the ligend Hmim according to the following Scheme 1. The effect of ligend Hmim concentration was examined using a concentration range from 1 to 10% in the carbon paste used for the preparation of modified electrode. By increasing the amount of Hmim concentration from 1 to 10 %, the oxidation peak current increased. So carbon paste modified by 10 % Hmim was used for further studies. The effect of accumulation time on the peak current of Pb(II) on the modified electrode was examined using different times ranged from 0 to 30s. By increasing the accumulation time, the peak current increased till reach a maximum value at 5s and after that the peak current showed a small decrease till 10s and after that the peak current become stable. The incensement in the peak current from 0s to 5s due the adsorption of Pb(II) on the electrode surface with time and more complex formed

between Pb(II) and Hmim till reach a maximum value and after that some of the outer adsorbed ions with a weak adsorption to the electrode leave the surface till a an equilibrium occurs.

The effect of potential scan rate on the electrochemistry of carbon CPME-Hmim was studied using  $5 \times 10^{-4}$  M Pb(II) in HCl 0.1 M. By increasing the scan rate values from 10 to 250 mV/s, the oxidation peak currents increased (Fig. 3a). Fig. 3b showed the relation between the anodic and cathodic peak current as a function in scan rate values. By increasing the scan rate values the anodic and cathodic peak current increased. Fig. 3c showed the effect of scan rate on the position of peak potential, where the anodic peak potential shifted to more positive values and the cathodic peak shifted to more negative values.



Scheme 1. The structure of the ligand mercapto-1-(2-isopropylphenyl)-imidazole (Hmim) and its lead(II) complex 1.



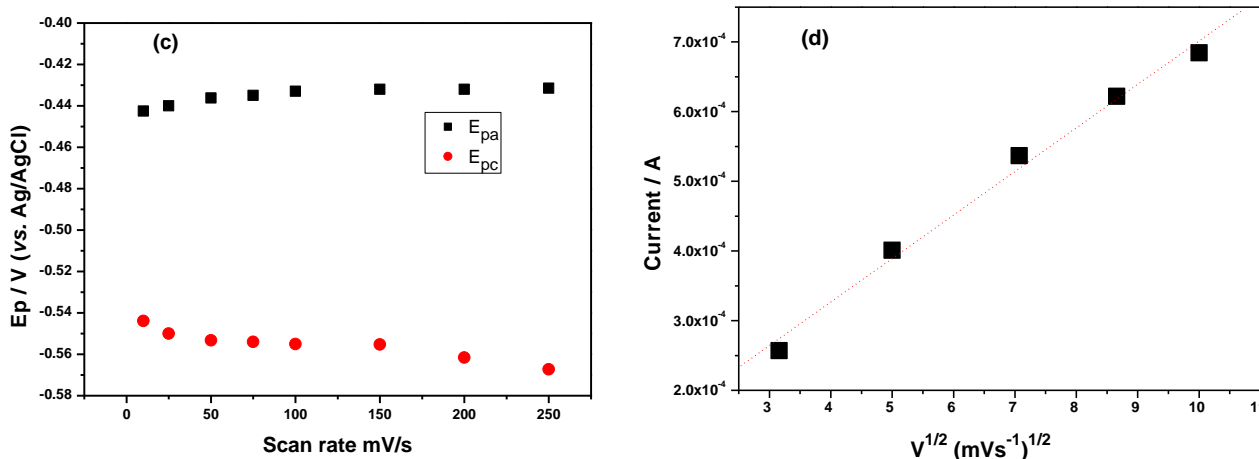
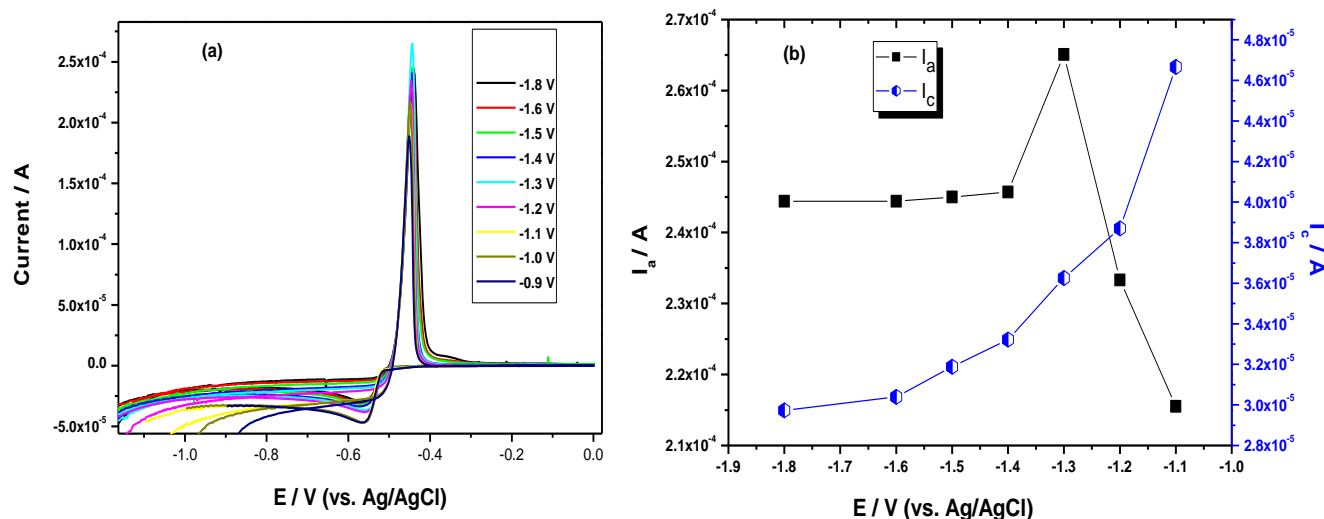


**Figure 3.** (a) The cyclic voltammograms for  $5 \times 10^{-4}$  M Pb(II) at different scan rate from 10 to 250 mV/s, using CPME-Hmim in 0.1 HCl M solution. (b) Plot  $I_p$  against scan rate for  $5 \times 10^{-4}$  M Pb(II). (c) Plot  $E_p$  against scan rate for  $5 \times 10^{-4}$  M Pb(II). (d) Plot of anodic peak current  $I_p$  for  $5 \times 10^{-4}$  M Pb(II) vs.  $v^{1/2}$ .

The oxidation peak currents for  $5 \times 10^{-4}$  M Pb(II) were proportional to the square root of the scan rate ( $v^{1/2}$ ) (Fig. 3d) using scan rate values from 10 to 100 mV/s, which, indicates that the electron transfer reaction is diffusion controlled [44]. The linear regression equation was  $I_p$  (A) =  $7.689 \times 10^{-5} + 6.246 \times 10^{-5} v^{1/2}$  with a 0.99 correlation coefficient and  $1.9 \times 10^{-5}$  standard deviation (SD).

Plotting the relation between the obtained peak potentials and  $\log v$  for  $5 \times 10^{-4}$  M Pb(II), a linear relation was obtained using potential scan rate from 10 to 100  $\text{mV s}^{-1}$ . Such behavior reveals the irreversible nature of the electrochemical process for lead.

### 3.4. Effect of initial potential on the peak current height



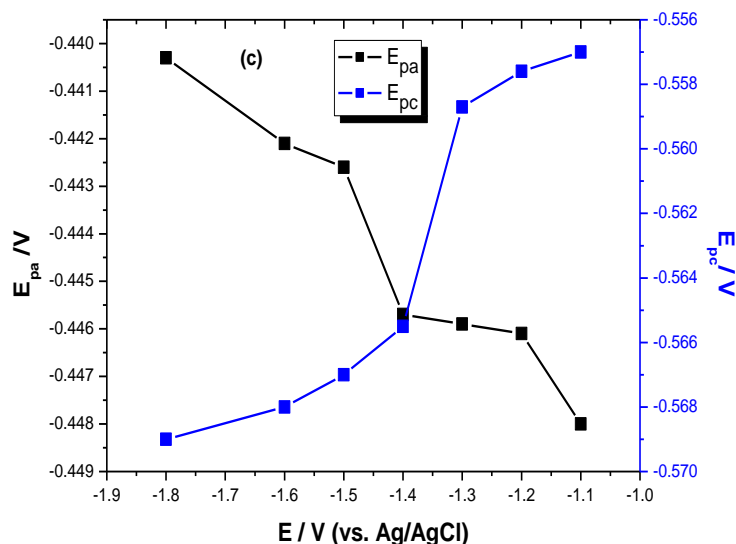


**Figure 4.** (a) Cyclic voltammograms for  $5 \times 10^{-4}$  M Pb(II) at different initial potentials, (b) The effect of initial potential on the anodic and cathodic peak current height of  $5 \times 10^{-4}$  M Pb(II) and (c) The effect of initial potential on the anodic and cathodic peak position of  $5 \times 10^{-4}$  M Pb(II).

The effect of initial potential on the anodic and cathodic peak current height of  $5 \times 10^{-4}$  M Pb(II) was investigated using a wide range of potential from - 1.8.0 V to - 0.9 V using cyclic voltammetry (Fig. 4a). For anodic peak current, by increasing the initial potential to more positive value the peak current increased to reach a maximum current value at - 1.3 V, while for cathodic peak current, the peak height increased by increasing the initial potential to more positive value (Fig. 4b). The effect of initial potential on the peak position was also examined (Fig. 4c). For anodic and cathodic peak potentials, by increasing the initial potential to more positive value the anodic and cathodic peak potentials were shifted to more negative values.

### 3.5. Squar wave voltammetric studies

#### 3.5.1. Effect of supporting electrolyte and pH

The effect of pH on the electrochemical behavior of Pb(II) using CPME-Hmim was studied using square wave voltammetric techniques in the pH range of 2.0 to 11.7 using 0.1 M BR buffer.

The oxidation peak of Pb(II) showed the highest peak current and best peak shape at pH 1.0. The effect of supporting electrolytes was also investigated to study the electrochemical oxidation of Pb(II). 0.1 M of different supporting electrolytes were examined such as  $\text{CH}_3\text{COOH}$ ,  $\text{H}_3\text{PO}_4$ ,  $\text{H}_3\text{BO}_3$ ,  $\text{H}_2\text{SO}_4$ ,  $\text{HClO}_4$ ,  $\text{HNO}_3$  and  $\text{HCl}$ . CPME-Hmim showed a best oxidation peak in the presence of  $\text{HClO}_4$ ,  $\text{HNO}_3$  and  $\text{HCl}$  solutions. The highest peak current and the best peak shape for the oxidation of Pb(II) were observed using 0.1 M  $\text{HCl}$  solution. So for further work a 0.1 M  $\text{HCl}$  buffer was selected for further studies.

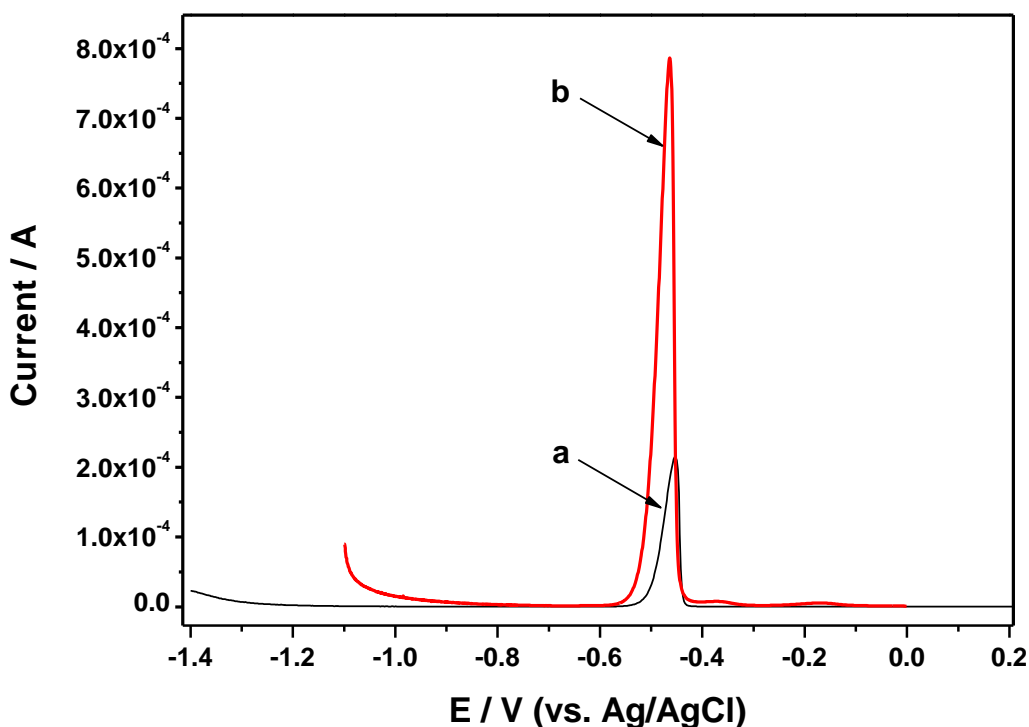


**Figure 5.** The square wave voltammograms for Pb(II) using a bare carbon paste electrode (CPE) (a) and carbon paste electrode modified with N-isopropyl-2-thioimidazole (CPME-Hmim)

Fig. 5 showed the square wave voltammograms for Pb(II) using a bare CPE (a) and CPME-Hmim (b). It is clear that the anodic peak current for Pb(II) in the presence of a CPME-Hmim is much higher than the peak current of Pb(II) in case of a bare CPE. This enhancement in the oxidation peak current due to the increase of Pb(II) concentration in the electrode surface by the complex formation between Pb(II) and Hmim as mentioned before.

### 3.5.2. Effect of square wave voltammetric parameters

The effect of different square wave voltammetric parameters was examined on the peak height of  $5 \times 10^{-4}$  M Pb(II). Fig. 6a shows the influence of square wave frequency on the peak current of  $5 \times 10^{-4}$  M Pb(II) using different values from 8 to 15 Hz. By increasing the square wave frequency, the peak current increased. A linear part was observed from 8 to 11 Hz square wave frequency. Thus for further study, the 11 Hz square wave frequency was selected for further investigations.

The effect of square wave pulse amplitude on the peak current of  $5 \times 10^{-4}$  M Pb(II) using 11 Hz square wave frequency is shown in Fig. 6b. The pulse amplitude ranged from 1.0 to 50 mV. The peak current increased linearly from 1.0 to 20 mV. Therefore, a 20 mV will be the optimum square wave pulse amplitude height and will be used in the next work.

The last square wave parameter examined was the step potential. The effect of step potential (0.5 - 5 mV) on the peak height of  $5 \times 10^{-4}$  M Pb(II) is depicted using 11 Hz square wave frequency

and 20 mV square wave pulse amplitude and the other experimental parameters as shown in Fig 2b. As the step potential increases, the peak height increases linearly up to 3 mV, after that the increasing in the peak height is not pronounced (Fig. 6c). So step potential with 3 mV was selected for further studies.

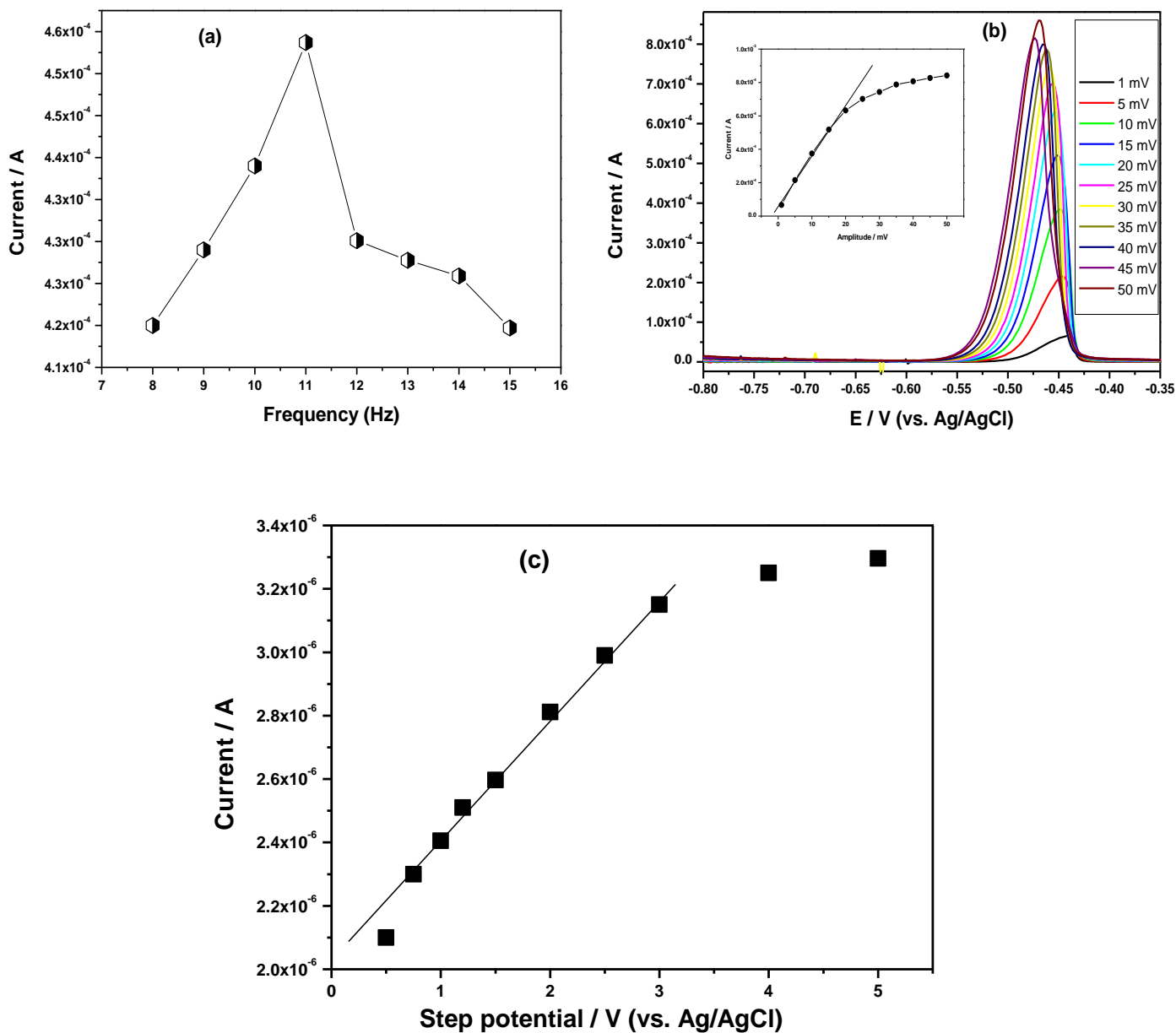


**Figure 6.** (a) The influence of square wave frequency on the peak current of  $5 \times 10^{-4}$  M Pb(II) using different values from 8 to 15 Hz. (b) The effect of square wave pulse amplitude on the peak current of  $5 \times 10^{-4}$  M Pb(II) using 11 Hz square wave frequency. (c) The effect of step potential (0.5 - 5 mV) on the peak height of  $5 \times 10^{-4}$  M Pb(II) using 11 Hz square wave frequency and 20 mV square wave pulse amplitude and the other experimental parameters as mentioned in the text.

3.5.3. Effect of Initial potential

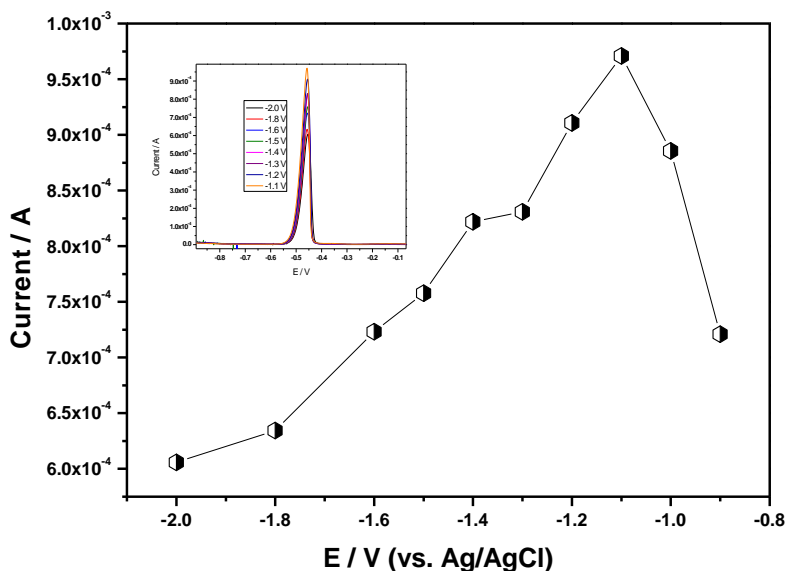


Figure 7. The effect of initial potential on the peak current height of 5x10<sup>-4</sup> M Pb(II).

The effect of initial potential on the peak current height of 5x10<sup>-4</sup> M Pb(II) was investigated using a wide range of potential from -2.0 V to -0.9 V using 11 Hz square wave frequency, 20 mV square wave pulse amplitude and 3 mV step potential. As shown from Fig. 7 by increasing the initial potential to more positive values, the peak current for 5x10<sup>-4</sup> M Pb(II) increased to reach a maximum value at -1.1 V after that the peak current decreased. So, -1.1 V was selected as an initial potential for further studies.

3.6. Calibration curve and Detection limit

Table 1. Detection limits (LOD) of Pb(II) using the proposed method and the methods from literature.

Technique	LOD	Reference
Square wave voltammetry	3.18 × 10 <sup>-8</sup> M	The present work
Differential pulse stripping voltammetry	8x10 <sup>-9</sup> M	27
Square wave voltammetry	7.68x10 <sup>-10</sup> M	31
Differential pulse stripping voltammetry	4.0x10 <sup>-8</sup> M	32
Differential pulse stripping voltammetry	0.8 ug/L	37

To examine the readability of the prepared electrode under investigation, the following optimum conditions were used for the square wave determination of Pb(II): 0.1 M HCl buffer, 11 Hz square wave frequency, 50 mV square wave pulse amplitude and 3 mV step potential.

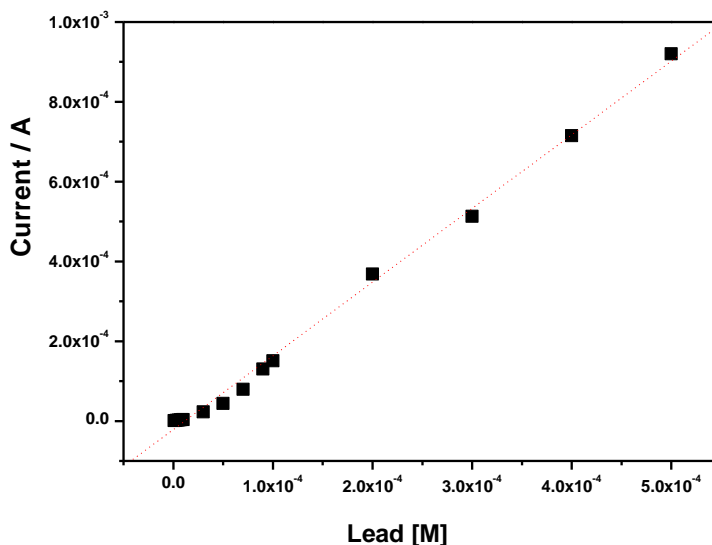


**Figure 8.** Calibration plots for different Pb(II) concentration from  $1 \times 10^{-6}$  M to  $1 \times 10^{-3}$  M using the optimum conditions mentioned in text.

The effect of concentration on the peak current of Pb was examined from  $1 \times 10^{-6}$  M to  $1 \times 10^{-3}$  M, the resulted calibration curve showed a linear range from  $1 \times 10^{-6}$  to  $5 \times 10^{-4}$  M with a correlation coefficient of 0.9991 and a relative standard deviation (RSD) of  $1.831 \times 10^{-5}$  (Fig. 8). The lower detection limit for Pb(II) was calculated based on three signal to noise ration and it was found to be  $3.18 \times 10^{-8}$  M. The obtained value for lower detection limit in this method was compared with the values from the different electrochemical methods sited in literature and the data was given in Table 1.

### 3.7. Reproducibility

To examine the readability of the prepared electrode under investigation, the produced peak current of  $5 \times 10^{-4}$  M Pb(II) using the optimum conditions mentioned above was examined by successive ten measurements. The RSD was calculated and it was found to be 3.56%, and this value indicates that this method gives a good reproducibility for the obtained results.

### 3.8. Effect of Interferences

The effect of some metal ions such as  $\text{Cu}^{++}$ ,  $\text{Cd}^{++}$  and  $\text{Zn}^{++}$  as the most interfering ions in the electrochemical determination Pb(II) was examined. Different  $\text{Cu}^{++}$  concentrations ranged from  $1 \times 10^{-5}$  to  $1 \times 10^{-3}$  M was added to  $5 \times 10^{-4}$  M Pb(II). From  $1 \times 10^{-5}$  to  $1 \times 10^{-4}$  M  $\text{Cu}^{++}$  no effect on  $5 \times 10^{-4}$  M  $\text{Pb}^{++}$  and no signals for  $\text{Cu}^{++}$  was observed, while addition of  $1 \times 10^{-4}$  M  $\text{Cu}^{++}$  showed a small signal at about

-0.15 V and has no effect of the peak current of Pb(II). Addition of a different concentrations ranged from  $1 \times 10^{-5}$  to  $1 \times 10^{-4}$  M  $\text{Cd}^{++}$  showed no effect on the peak current of on  $5 \times 10^{-4}$  M Pb(II), while  $5 \times 10^{-4}$  M of  $\text{Cd}^{++}$  decreased the peak current of  $5 \times 10^{-4}$  M Pb(II) by about 0.62 %. Addition a concentration range from  $1 \times 10^{-5}$  to  $1 \times 10^{-3}$  M  $\text{Zn}^{++}$  showed no effect on the peak current of on  $5 \times 10^{-4}$  M Pb(II).

### 3.9. Analytical Applications

**Table 2.** Determination of Pb(II) in water samples by the proposed method (n=5) and from a standard method (ICP-AES)

No. of sample	Pb(II) added[M]	Pb(II) found[M]	Recovery(%)	Pb(II) from ICP-AES [M]
1	$1 \times 10^{-6}$	$1.028 \times 10^{-6}$	102.8	$1.1 \times 10^{-6}$
2	$3 \times 10^{-6}$	$2.96 \times 10^{-6}$	98.67	$2.75 \times 10^{-6}$
3	$5 \times 10^{-6}$	$5.19 \times 10^{-6}$	103.8	$5.02 \times 10^{-6}$
4	$7 \times 10^{-6}$	$7.19 \times 10^{-6}$	102.74	$7.24 \times 10^{-6}$
5	$9 \times 10^{-6}$	$9.55 \times 10^{-6}$	106.11	$9.06 \times 10^{-6}$
6	$1 \times 10^{-5}$	$1.058 \times 10^{-5}$	105.8	$1.014 \times 10^{-5}$
7	$5 \times 10^{-5}$	$5.22 \times 10^{-5}$	104.4	$5.024 \times 10^{-5}$

In order to test the validity of the prepared CPME-Hmim the proposed method was applied for the electrochemical determination of Pb(II) in different water samples. The samples were prepared by addition different concentrations from a standard Pb(II) to drinking water samples. Using the optimum conditions and calibration curve (analytical equation:  $y = -2.129 \times 10^{-5} + 1.847x$ ) the obtained results are represented in Table 2. The recovery ranges between 98.67-106.11%. The obtained results were compared with the data obtained from the ICP-AES instrument (Table 2). From Table 2 the obtained results from the prepared modified electrode were well agreed with those obtained from ICP-AES method.

## 4. CONCLUSIONS

- A thione-containing ligand N(2-isopropylphenyl)-2-thioimidazole (Hmim) and its Pb(II) complex was prepared and characterized.
- A carbon paste electrode modified by the ligand Hmim was constructed and characterized by SEM-EDEX and cyclic voltammetry.
- The electrochemical behavior of Pb(II) ions was studied at the surface of both bare carbon paste electrode CPE and its modified one CPME-Hmim.
- Optimization the experimental conditions for the determination of Pb(II) ions using square wave voltammetry at the surface of the constructed CPME-Hmim.

- Application of this method for the electrochemical determination of Pb(II) ions in different water samples and compared the obtained data with a standard ICP-AES method.

#### ACKNOWLEDGEMENTS

This work was financial supported by Taif University, under the project number 1269/432/1.

#### References

1. M.G.A. Korn, G.L. Santos, S.M. Rosa, L.S.G. Teixeira and P.V. Oliveira, *Microchem.*, J. 96 (2010) 12.
2. R. Dobrowolski, A. Adamczyk and M. Otto, *Talanta*, 82 (2010) 1325.
3. J.C. Lam, K. Chan, Y. Yip, W. Tong and D.W. Sin, *Food Chem.*, 121 (2010) 552.
4. F.A. Aydin and M. Soylak, *J. of Hazard. Mater.*, 173 (2010) 669.
5. J. Otero-Roman, A. Moreda-Pineiro, P. Bermejo-Barrera, A. Martin-Esteban, *Talanta*, 79 (2009) 723.
6. K. Ndung, S. Hibdon and A.R. Flegal, *Talanta*, 64 (2004) 258.
7. V. Arancibia, E. Nagles and S. Cornejo, *Talanta*, 80 (2009) 184.
8. A.A. Ensafi, T. Khayamian, A. Benvidi and E. Mirmomtaz, *Anal. Chim. Acta*, 561 (2006) 225.
9. M.C.V. Mamani, L.M. Aleixo, M. Ferreira de Abreu and S. Rath, *J. of Pharm. Biomed. Anal.*, 37 (2005) 709.
10. E. Shams, A. Babaei and M. Soltaninezhad, *Anal. Chim. Acta*, 501 (2004) 119.
11. E. Nagles, V. Arancibia and R. Ríos, *Int. J. Electrochem. Sci.*, 7 (2012) 4545.
12. J. Jakmunee and J. Junsomboon, *Talanta*, 77 (2008)172 .
13. J. Zen and J. Wu, *Anal. Chem.*, 68 (1996) 3699.
14. R. A.A. Munoz and L. Angnes, *Microchem. J.*, 77 (2004) 157.
15. S. Laschi, I. Palchetti and M. Mascini, *Sens. Actuators B*, 114 (2006) 460.
16. G. Hwang, W. Han, J. Park and S. Kang, *Sens. Actuators B*, 135 (2008) 309.
17. B. Bas and M. Jakubowska, *Anal. Chim. Acta*, 615 (2008) 39.
18. G. Hwang, W. Han, S. Hong, J. Park and S. Kang, *Talanta*, 77 (2009) 1432.
19. Y. Li, X. Liu, X. Zeng, Y. Liu, X. Liu, W. Wei and S. Luo, *Sens. Actuators B*, 139 (2009) 604.
20. W. Li, G. Jin, H. Chen and J. Kong, *Talanta*, 78 (2009) 717.
21. M.A. El Mhammedi, M. Achak, M. Bakasse and A. Chtaini, *Chemosphere*, 76 (2009) 1130.
22. R. Nasraoui, D. Floner, C. Paul-Roth and F. Geneste, *J. Electroanal. Chem.*, 638 (2010) 9.
23. H. Zejli, K. R. Temsamani and J. L. Hidalgo-Hidalgo de Cisneros, I. Naranjo-Rodriguez, P. Sharrock, *Electrochem. Commun.*, 8 (2006) 1544.
24. K.C. Honeychurch, J.P. Hart and D.C. Cowell, *Anal. Chim. Acta*, 431 (2001) 89.
25. K.C. Honeychurch, J.P. Hart, D.C. Cowell and D.W.M. Arrigan, *Sens. Actuators B*, 77 (2001) 642.
26. S. Yuan, W. Chen and S. Hu, *Talanta*, 64 (2004) 922.
27. H. Zheng, Z. Yan, H. Dong and B. Ye, *Sens. Actuators B*, 120 (2007) 603.
28. R.O. Kadara and I.E. Tothill, *Anal. Chim. Acta*, 623 (2008) 76.
29. J.C. Cypriano, M.A.C. Matos and R.C. Matos, *Microchem. J.*, 90 (2008) 26.
30. S. Senthilkumar and R. Saraswathi, *Sens. Actuators B*, 41 (2009) 65.
31. M.A. El Mhammedi, M. Achak and A. Chtaini, *J. Hazard. Mater.*, 161 (2009) 55.
32. I. Cesarino, G. Marino, J. Matos and E.T. Cavalheiro, *Talanta*, 75 (2008) 15.
33. W. Yantasee, Y. Lin, G.E. Fryxell and B.J. Busche, *Anal. Chim. Acta*, 502 (2004) 207.
34. C. Hu, K. Wu and X. S. Hu, *Talanta*, 60 (2003) 17.
35. M.F. Mousavi, A. Rahmani, S.M. Golabi, M. Shamsipur and H. Sharghi, *Talanta*, 55 (2001) 305.

36. R.Y.A. Hassan, I.H.I. Habib and H.N.A. Hassan, *Int. J. Electrochem. Sci.*, 3 (2008) 935.
37. E.S. Claudio, H.A. Godwin and J.S. Magyar, *Prog. Inorg. Chem.*, 51 (2003) 1.
38. G. A. M. Mersal and M.M. Ibrahim, *Int. J. Electrochem. Sci.*, 6 (2011) 761.
39. R. Shunmugam and D. Sathyanarayana, *J. Coord. Chem.*, 12 (1983) 151.
40. E.S. Raper and J.L. Books, *J. Inorg. Nucl. Chem.*, 39 (1977) 2163.
41. L.J. Bellamy, *The Infrared Spectra of Complex Molecules*, 3rd ed. (Chapman and Hall, London (1975).
42. E.S. Raper and P.H. Crackett, *Inorg. Chim. Acta*, 50 (1981) 159.
43. A.A. Isab and M.I.M. Wazeer, *J. Coord. Chem.*, 58 (2005) 529.
44. Umesh Chandra, B.E. Kumara Swamy, Ongera Gilbert, S. Sharath Shankar, K.R. Mahanthesha and B.S. Sherigara, *Int. J. Electrochem. Sci.*, 5 (2010) 1.